Nanostructured Acetylcholinesterase (ACHE) Memristor/Memcapacitor Mimicks *Brachyhypopomus* Electric Fish's Signal-Cloaking Behavior

E. T. Chen[1*] and J. Thornton[2]
[1]Advanced Biomimetic Sensors, Inc., 13017 Wisteria Dr, #109, Germantown, MD 20874; [2] Bruker Nano, 19 Fortune Dr., Billerica, MA 01821, * To whom it should be contacted: ellenchen@nanobiomimeticsensors.com,

ABSTRACT

The Brachyhypopomus Electric (BHE) fish is known for its *signal-cloaking* behavior that allows it to avoid predators by shifting its electroreceptive pulses from low frequency to less detectable high-frequency through a phase-delay "head-tail" *Electric Organ Discharge* (EOD) with an energy saving consumption. We report a new type of Memristor/Memcapacitor device that performs signal-cloaking, which mimics BHE's behavior based on a self-assembled nanoisland structured biomimetic acetylcholinesterase (ACHE) gorge Membrane Electrode Assembling (MEA) on a gold electrode, another MEA has a "flat bridge"/nanopore membrane. The device has an asymmetric engineering design that allows electron nonlinear tunneling as Memcapacitor #1. Memcapacitor #2 was made of a mutated gorge of ACHE, which renders the device unable to perform signal-cloaking. We observed the memcapacitor #2 has a disturbed circular current with toroidal movement forming a nonferroelectromagnetic field with orders of magnitude enhancement of electric charge over various phases from 45 to 315^0 was observed. By comparing the results of discharges at 25 and 1000 Hz, the "*BHE"* fish reduced the energy consumption by 14% and 33% by emitting "head-tail" "EOD" at 1 kHz, respectively.

***Key Words*:** Nanobiomimetic Acetylcholinesterase (ACHE) Memcapacitor; Circular Current; Signal-Cloaking; Asymmetric Engineering; Toroid Movement; Multiple-Organ Biphase Frequency Switch; Electric Organ Discharge (EOD); Hyppocampal-Neocortical Neuronal Network.

INTRODUCTION

Brachyhypopomus Electric (BHE) fish is known for its *signal-cloaking* behavior that allows it to avoid predators by shifting its electroreceptive pulses from low frequency to less detectable high-frequency through a phase-delay "head-tail" *Electric Organ Discharge* (EOD) with an energy saving consumption [1-3]. The BHE fish signal-cloaking strategy produces broad frequency electric field close to the body, causing its low frequency field to be cancelled by the local field, hence the predators are unable to find them. There is a risk of releasing huge amounts of heat during electrical discharge by the metal oxide thermal memcapacitors. This causes reduction in energy converting efficiency and is not beneficial for energy storage or for computing purposes. Special features of memcapacitors in negative and diverging capacitance received attention in the memristor/ mamcapacitor society [16-17]. Martinez-Rincon's group published an article emphasizing the utility of negative and diverging capacitance in computing: "The resulting memcapacitor exhibits not only hysteretic charge-voltage and capacitance-voltage curves but also both negative and diverging capacitance within certain ranges of the field, due to its simplicity and unusual capacitance features. We expect it to find use in both analog and digital applications." [17]. Our group developed the first nanomemcapcitor with negative and diverging capacitance made of non metal oxide materials and reached a superior performance in plasticity, elasticity, stability and high power and energy density without environmental pollution and current leaking [6-7].

Circular current induced by junctions of aromatic molecules of the delocalized molecules has drawn interest from theoretical scientists [18-19]. Scientists have envisioned its future applications. The goal of this research is to develop a memcapacitor device that performs signal-cloaking, which mimics BHE's behavior saving operational energy and enhancing the energy storage under the conditions of electrolyte-free, nature ACHE-free, metal oxide-free and reagent-free.

EXPERIMENTAL

Asymmetric Design of the Memcapacitors

An asymmetric design for the biomimetic ACHE hippocampus-neocortical neuronal memcapacitor is illustrated in Fig 1A. It was defined as "BHE fish", and it consists of a nanoisland self-assembling Membrane (SAM) Au/triacetyl-ß-cyclodextrin (T-CD), poly(4-vinylpyridine) (PVP) and Polyethylene glycol diglycidyl ether (PEG)/copolymer β-CD as one *Membrane Electrode Assembling* (MEA) separated by a insulator and connected with another MEA of Au. The monoimidazolyl derivative dimethyl ß-cyclodextrin (M-CD)/TCD/PVP/PEG/embedded with o-nitrophenyl acetate (o-NPA) through Pt current collectors at two ends. The insulator absorbed 1M methanol as model 1. The Atomic Force Microscopy (AFM) images and membrane fabrication methods were reported in

literature [8, 20]. An asymmetric design for the Biomimetic "Predator Fish" memcapacitor consisted of Au/MCD/TCD/PVP/PEG with structure of vertical bridge/nanopore MEA separated by an insulator and connected with a Au/MCD/TCD/PVP/PEG embedded with o-NPA forming flat bridge/nanopopore memcapacitor as model 2 shown in Figure 1B. The AFM images were reported in literature 20.

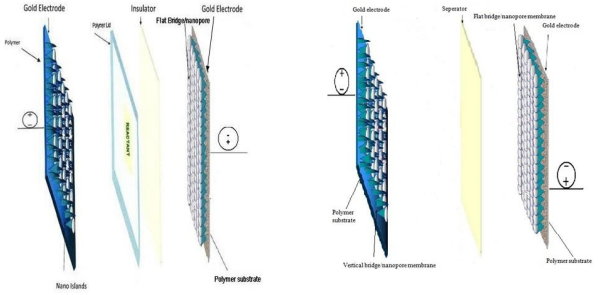

Fig 1A illustrates the Memcapacitor 1 model as a neuron network of "BHE"; Fig 1B illustrates Memcapacitor 2 as a neuron network for the "Predator".

Memcapacitor i-V Curves

Memcapacitor's characteristic i-V curves and the diverging frequency were studied using CV method at 20 mV/s scan rate in room temperature.

Circular Current (CC)

Circular current was identified through a continuous scan of each of the half memcapacitor cells for multiple cycles using CV method at a fixed scan rate. From the CV profiles results constructed a 3D contour mapping between the location of Direct Electron Transfer peaks (Z), switch point location (X) and peak current (Y).

Electromagnetic Field Induced by CC

Evaluation of electromagnetic field induced by CC was conducted by changing the connect angles between the anode separated by an insulator and the cathode (Pt) within the AU/MEA of vertical bridge/Nanopore cell from 45, 90, 180, 225, 270 to 315° clockwise horizontally in 1 M methanol at room temperature using a CV method. A modified Biot-Savert equation was used to calculate the overall magnetic field strength at each of the 6 angle changes.

Synapse Profiles

The whole cell synapse profiles during " Slow-Wave-Sleeping" (SWS) at 0.2 Hz (Delta wave) were studied at room temperature in 1 M methanol.

Assessing of the Energy Saving Through *Signal-Cloaking*

SC behavior was studied using whole memcapacitor cell for the two models at frequencies of 25 and 1000 Hz compared at room temperature. Ratio of action potential at 1kHz vs. at that of 25 Hz at the head and at the tail was compared for the power saving advantage of SC behavior compared with the two models.

Assessing Stability and Efficiency

The Double Step Chronopotentiometry (DSCPO) method was used for assessing utility of the newly developed memcapacitors in assessing stability and efficiency of the 9,999 discharge/charge cycles in 1M methanol at ± 30mA using the best performing frequency of 1 KHz for model 1, and best frequency of 0.25 Hz for model 2.

RESULTS AND DISCUSSIONS

Characterization of the Memristors

In Fig 2A the Au/"vertical/nanopore"/Pt MEA's peak increased dramatically as the total scan time increased over the 10 cycles. In contrast, when o-NPA is present, the current reduced to zero, indicating o-NPA played a role in the event. The i-V curves were switched and the DET peaks were observed. Fig 2B the red line show the typical memcapacitor i-V curve with a switch point near -0.2V, and the half cell of Au/nano island-insulator/Pt has a quarter of the peak intensity compared with in Fig 2A. The memristor's switch point was observed in the red line without an insulator. The exponential increase of the current in Fig 3 may be caused by an abnormal electric field (17).

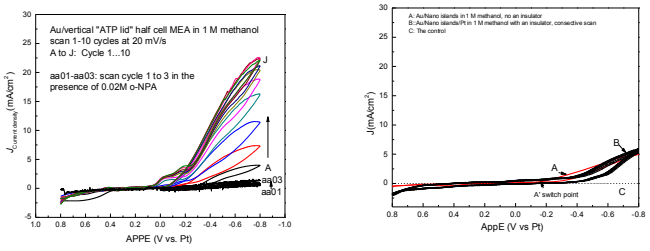

Fig 2A illustrates the AU/"vertical nanopore"/Pt half cell MEA with 10 cycle scan compared in the presence of o-NPA; Fig 2B is the half cell of Au/nanoisland/Pt MEA (black), and the half cell without an insulator (red).

The prefect hysteresis loops in the presence o-NPA and ACH using memristor #2 was observed in our report [22].

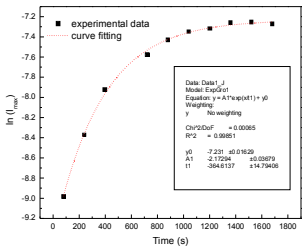

Fig 3 Illustrates the plot of current vs. time of the 10 cycle scans of the half cell of Au/"vertical bridge/nanpore" memcapacitor in 1M methanol.

Circular Current (CC)

The exponential increase of the current in Fig 3 indicates its Schottky diode behavior, i.e., a small potential drop at 0.1V from the origin and then increased nonlinearly that provides higher switching speed and system efficiency [21]. In contrast, CV curves from aa01 to aa03 are flat lines after added 0.02 M o-NPA. The larger peak from A to J was signed as the diode peak, and the small peak (located near 0.1V) was signed as the direct electron transfer (DET) peak in Fig 2A [20]. The observations of CC was shown in Fig 4B through plot of current vs. cycle numbers of DET peak and Switch point, respectively in Fig 4A. Delocalized electron relay through the multiple residue groups, hydrogen bounding and hydrophobic π-π staking could be the driving force [22]. The DET constant Ks was calculated at 107/s, and the diode peak is 192.5/s, and it may reach 220.2/s from the vector contributions from our calculation [23-25]. In Fig 4B, a disturbance of the CC momentum appearing at the left side corner was observed.

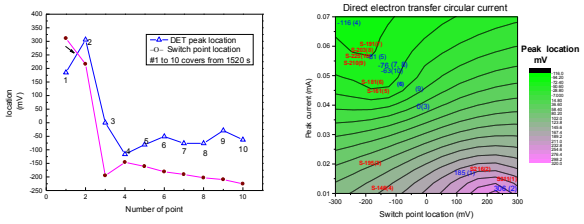

Fig 4A illustrates the plot of DET peak location and switch point location vs. number of cycles; and the Fig 4B shows the contour map.

Electromagnetic Field Induced by CC

Changing the connect angles between the anode and cathode within the AU/MEA of vertical bridge/nanopore from 45, 90, 180, 225, 270 to 315°, induced changes of current reflected in CV curves as shown in Figure 5A and 5B that confirmed CC's induction. The largest current is at 225° of 435 μA compared with other angles were much smaller.

The total magnitude of magnetic field can be calculated by using the Biot-Savart law [18]:

$$\vec{B} = \vec{B}_{inner} + \vec{B}_{outer} = \frac{\mu_0 I\theta}{4\pi}\left(\frac{1}{a} - \frac{1}{b}\right) \text{ (into page)}$$

Consider the current charging loop formed from radial lines and segments of circles whose centers are at point P, a is the inner radius, b is the out radius of the arc. θ is the angle of the current carrying arc. μ_0 is the permeability of free space, and I is current pass the arc. The induced magnetic field values are 0.00736, 0.0465, 0.2852, 1.683, 0.4644 and 0.0514 Tesla, at angles of 45, 90, 180, 225, 270 and 315°, respectively. The overall magnetic field strength induced by switch angels and by circular current can be calculated according to a modified equation:

$$B_{total} = B_c + B_{arc} = \mu_0 NI(2\pi r)^{-1} + B_{arc}$$

Here B_{arc} is defined by t

The Biot-Savert law, and B_c were defined by Ampere's law. Herein, the highest total value of magnetic field induced is 3.53 at 225°. As shown in Fig 5B, the quick raised current is at the quantum Femi Resonance point [18] at 225°. This is the first reported instance of an electromagnetic field induced by non ferromagnetic materials. Using NIST SRM965A human sera at glucose level 2 followed the same procedures applied onto this device, we confirmed the finding.

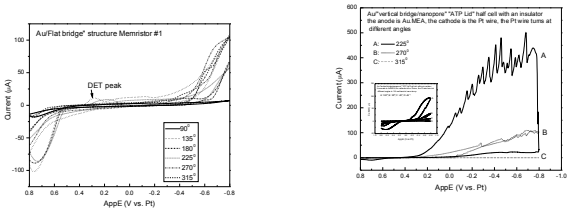

Fig 5A illustrates the Au/"Flat bridge/nanopore" "BHE" has a balanced i-V profiles at different turning angles; Fig 5B illustrates the AU/"vertical bridge/nanopore" "Predator" has a synchronized peak at 225°, insert is the angles change in the area of 45-180°.

Synapse Profiles

The electric synapse profile was presented in SWS Delta waves (0.2 Hz) in Fig 6. It is evidenced that the BHE fish has a great declarative memory consolidation with the highest wave intensity than the predator at night.

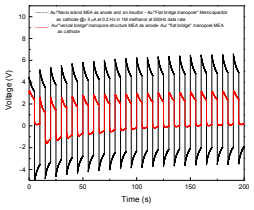

Fig 6 illustrates the comparison of synapse profiles between "BHE" fish (black) and "Predator" fish (red) at Delta SWS sleeping (0.2 Hz) in 1M methanol;

Assessing of the Energy Saving Through *Signal-Cloaking*

BHE fish's flexibility of signal-cloaking jumping from low to high frequency was mimicked by our Biomimetic BHE fish as shown in Fig 7A from 25 Hz to 1000Hz, and the energy saving at high frequency was demonstrated in Fig 7B by 16-33% compared at 25 Hz at head and tail, respectively.

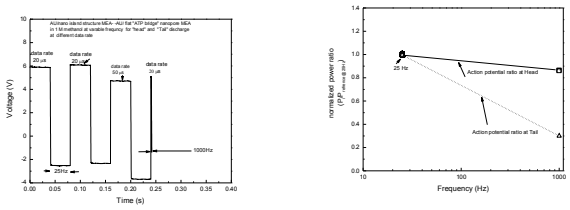

Fig 7A illustrates the "Healthy BHE fish" discharges at diverging frequency 25Hz -1 KHz and saved energy up to 33% compared at 25 Hz as shown in Fig 7B.

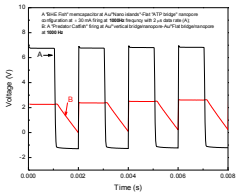

Fig 8 illustrates the "Predator catfish" discharges at 1 KHz with monophase firing (red); but the "BHE fish" can use head-tail biphase firing (black) at1 KHz.

Assessing Stability and Efficiency

In Figure 9, the curve A referred to the "BHE fish", it illustrates the stability and efficiency of model 1 memcapacitor for 9,999 cycles firing with 2 ms/cycle at ± 30 mA at 1KHz. It reached an average 100.0 ± 0.01% efficiency against the original starting point (as 100.0) compared with curve B of 98%, except starting several cycles are above 100%. Curve B refers to "predator" had 4s/cycle at ± 30 mA at 0.25 Hz.

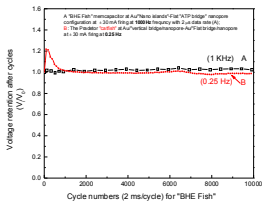

Fig 9 illustrates the efficiency of the discharge/charge cycle. Black line is the "BHE fish"; Red line is the "Predator fish".

CONCLUSION

The Biomimetic "BHE fish" avoidance of the "predator" by signal-cloaking was demonstrated.

ACKNOWLEDGEMENT

We thank Kevin Bowen for review of the manuscript.

REFERENCES

1. Stoddard PK and Markham MR, *Bioscience*, 58(5), 415-425, 2008.
2. Stoddard PK, Nature 400, 254-256, 1999.
3. Herberholz J and Marquart GD, Neurosci. 6, 125, 2012.
4. Sussman JL, Harel M, Frolow F, Oefner C, Goldman A, Toker L, Silman I, Science *253, 872-879, 1991;*
5. Whyte KA, Greenfield SA. Exp Neurol 184,496-509, 2003.
6. Chen ET, Ngatchou C, Sensors and Transducers J, 15, special, 42-48, 2012.
7. Chen ET, Ngatchou C, Clean Tech, 202-205, **2012.**
8. Thornton J, Christelle C, Chen T, Cleantech, 356-359**,** 2013**.**
9. Martinez-Rincon J and Pershin YV, Electron Devices, IEEE Transactions 58 (6), 1809–1812, 2011.
10. Martinez-Rincon J, Ventra MD, Pershin YV, Physical Review *B, 81(19),* 195430-1-195430-7, 2010.
11. Pickett MD, Medeiros-Ribeiro G and Williams RS, Nature Materials, DOI: 10.1038/NMAT3510, 2012.
12. Kozma, Pino RE, Pazienza GE, *Advances in neuomorphic memristor science and applications*, Springer publisher, 2012.
13. Ventra MD, Pershin YV, *On the physical properties of memristive, memcapacitive, and meminductive systems,* Nanotechnology 24, 255201, 2013.
14. Ohno T, Hasegawa T, Tsuruoka T, Terabe K, Gimzewski JK, Nature Materials, 10, 591-595, 2011
15. Yang JJ, Strukov DB, Stewart DR, Nature Nanotechnology 240, 2012. DOI:10.1038.
16. http:en.wikipedia.org, Negative resistance.
17. Martinez-Rincon J, Ventra MD, Pershin YV, Physical Review B*, 81(19),* 195430-1-195430-7, 2010.
18. Rai D, Hod O and Nitzan A, J. Physical Chemistry Letters, 2, 2118, 2011.
19. Islas R, Heine T and Merino G, Accounts of Chemical Research, 45(2), 215, 2012.
20. Chen ET, *Nanopore structured electrochemical biosensor,* US Patent 8,083,926, December 27, 2011.
21. Idea Diode, http:en.wikipedia.org
22. Chen ET, Thornton J, Ngatchou C, Duh SH, Nanotech 2014, in press.
23. E. Laviron, J. Electroanal Chem., 101, 19-28, 1979.
24. E. T. Chen, J. Thornton, C. Ngatchou, S-H. Duh, P.T. Kissinger, NSTi-Nanotech (3), 115-118, 2013.
25. Chen ET, *first volume, Third Edition,* Lyshevski SE Dekker Encyclopedia of Nanoscience and Nanotechnology, *CRC*, March 20, 2014.